Nuclear Matter Distributions in ^{6}He and ^{8}He from Small Angle *p*-He Scattering in Inverse Kinematics at Intermediate Energy

G. D. Alkhazov,[1] M. N. Andronenko,[1] A. V. Dobrovolsky,[1] P. Egelhof,[2] G. E. Gavrilov,[1] H. Geissel,[2] H. Irnich,[2] A. V. Khanzadeev,[1] G. A. Korolev,[1] A. A. Lobodenko,[1] G. Münzenberg,[2] M. Mutterer,[3] S. R. Neumaier,[3] F. Nickel,[2] W. Schwab,[2] D. M. Seliverstov,[1] T. Suzuki,[2] J. P. Theobald,[3] N. A. Timofeev,[1] A. A. Vorobyov,[1] and V. I. Yatsoura[1]

[1]*Petersburg Nuclear Physics Institute (PNPI), 188350 Gatchina, Russia*
[2]*Gesellschaft für Schwerionenforschung (GSI), 64291 Darmstadt, Germany*
[3]*Institut für Kernphysik (IKP), TH-Darmstadt, 64289 Darmstadt, Germany*

(Received 2 December 1996)

Differential cross sections for p-^{6}He and p-^{8}He elastic scattering have been measured in inverse kinematics at small momentum transfers up to $|t| = 0.05$ (GeV/c)^2 and projectile energies of about 700 MeV/nucleon. Nuclear matter densities deduced from the data are consistent with the concept that ^{6}He and ^{8}He nuclei have an α-like core and a significant neutron skin. The rms radii of the nuclear matter distributions were determined to be R_m (^{6}He) $= 2.30 \pm 0.07$ fm and R_m (^{8}He) $= 2.45 \pm 0.07$ fm. [S0031-9007(97)02737-3]

PACS numbers: 21.10.Gv, 25.40.Cm, 25.60.Dz, 27.20.+n

After the discovery of light neutron rich nuclei which exhibit an extended neutron distribution surrounding a nuclear core (e.g., ^{11}Li, ^{14}Be), various methods were applied to study this new type of nuclear structure [1]. The radii of such nuclei, in particular, were deduced from measured total reaction cross sections [2]. However, as known from studies of stable nuclei [3], the most accurate and detailed information on the nuclear matter distributions is obtained from proton elastic scattering at intermediate energies of about 1 GeV. This method can be applied also to study unstable exotic nuclei by measuring elastic cross sections in inverse kinematics, using radioactive beams and a hydrogen target. As theoretical considerations have shown [4], proton scattering at small momentum transfer is sensitive to the halo- or skin-like structures of nuclei, and from differential cross sections measured with high accuracy at small scattering angles the overall nuclear size can be determined precisely, and information on the shape of the radial distribution of nuclear matter may be obtained as well. The first experiment on the elastic scattering of light exotic nuclei on protons at intermediate energies was recently performed at the GSI, Darmstadt. Here we present the results of this experimental study on the neutron rich nuclei ^{6}He and ^{8}He. The p-^{4}He elastic cross section was also measured as a consistency check of the method. The experimental procedure and some preliminary results were reported elsewhere [5,6].

Differential cross sections $d\sigma/dt$ for proton elastic scattering were measured at the heavy-ion synchrotron (SIS) using secondary ^{4,6,8}He beams with incident kinetic energies of 699, 717, and 674 MeV/nucleon, respectively. These beams were produced by fragmentation of ^{18}O ions from the SIS impinging on a beryllium target and were isotopically separated by the fragment separator FRS [7]. The intensity of the secondary beams was about 10^3 s^{-1} in all cases. The experimental setup is displayed in Fig. 1. The helium projectiles interacted with protons inside the hydrogen filled ionization chamber IKAR which served simultaneously as gas target and recoil detector. It was developed at the PNPI and was previously used for studying small-angle hadron elastic scattering [8,9]. IKAR ensures a sufficiently high H_2 target thickness (about 3×10^{22} protons/cm^2), and has a 2π acceptance in azimuthal angle for recoil proton registration. It operates at a pressure of 10 bars and consists of six identical modules [9]. Each module contains an anode plate, a cathode plate, and a grid, all electrodes being arranged perpendicular to the beam direction. The signals from the electrodes, registered by flash analog-to-digital converters, provide the energy of the recoil proton, or its energy loss in case it leaves the active volume, the scattering angle of the recoil proton, and the coordinate of the interaction point in the grid-cathode space. The four momentum transfer squared t was determined with the IKAR chamber in the range $|t| \leq 0.01$ (GeV/c)^2, with a resolution of about 0.0001 (GeV/c)^2. Between 0.01 and 0.05 (GeV/c)^2, $|t|$ was determined from the projectile scattering angle Θ, with a resolution of $0.002P\sqrt{|t|}$, where P is the projectile momentum. The angle Θ was measured by the tracking detector consisting of four two-dimensional multiwire proportional chambers (see Fig. 1). The scintillation counters

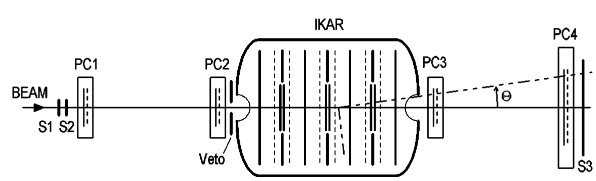

FIG. 1. Schematic view of the experimental setup. IKAR: multiple ionization chamber [9]; PC1–PC4: multiwire proportional chambers; S1–S3, VETO: scintillation counters. Tracks for a typical scattering event are shown by dot-dashed line.

S1, S2, S3, and Veto were used for triggering and for selecting projectiles that entered IKAR along its central axis within an area of 2 cm in diameter, defined by the Veto detector. Furthermore, the scintillation counters were used for beam particle identification via time-of-flight and dE/dx measurements.

The events corresponding to elastic scattering were selected by using the correlation of the proton recoil energies measured in IKAR with the corresponding values evaluated from the projectile scattering angles Θ [6]. Background events were observed to be randomly distributed outside this correlation and could be subtracted straightforward. The subtracted background amounts to 1.5%–7% for different t bins. The resulting cross sections are displayed in Fig. 2, with plotted error bars denoting statistical uncertainties only. The absolute normalization obtained is accurate within $\pm 3\%$. This number includes the uncertainties in beam monitoring, in the evaluation of the effective target thickness, and in the determination of the absolute value of the momentum transfer. The t scale was calibrated according to Ref. [9], with signals from ^{241}Am α sources which were deposited on each cathode plate of IKAR. An alternative procedure which uses the measured projectile scattering angle Θ gave a consistent result. The uncertainty in the t-scale calibration is estimated to be $\pm 1.5\%$. The measured p-^{4}He cross section (Fig. 2) is in close agreement with previous data [10], obtained in direct kinematics.

For deducing information on the nuclear density distributions in ^{6}He and ^{8}He from the measured cross sections, the Glauber multiple scattering theory was applied. Calculations were performed using the basic Glauber formula for proton-nucleus elastic scattering (see, e.g., Ref. [3]). Only the scalar part of the elementary proton-nucleon scattering amplitude was taken into account, which was described by the standard high-energy parametrization with an exponential t dependence [3]. The relevant quantities used as an input are: the total proton-proton (pp) and proton-neutron (pn) cross sections, the ratios of the real to the imaginary parts of the pp and pn amplitudes (these values being evaluated from experimental data and phase shift analyses for free pp and pn scattering), and the slope parameters β_{pp} and β_{pn}. The latter ones were chosen to be $\beta_{pp} = \beta_{pn} = 0.17$ fm^2. This particular value gives the best description of the p-^{4}He differential cross section (Fig. 2), with a matter radius of ^{4}He of 1.49 fm which corresponds (after taking into account the charge form factors of the proton and the neutron) to the experimentally determined ^{4}He charge radius of 1.67 fm [11]. Also, this value for β is close to those used in the literature for the analysis of proton-nucleus scattering at these energies [3]. The ground-state many-body nuclear densities were taken as products of one-body densities. Center-of-mass correlations were taken into account according to Eq. (4.12) of Ref. [3].

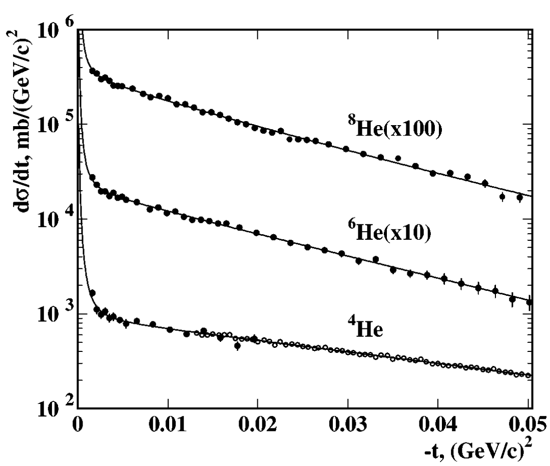

FIG. 2. Absolute differential cross sections $d\sigma/dt$ versus the four momentum transfer squared, for p-^{4}He, p-^{6}He, and p-^{8}He elastic scattering measured in the present experiment (full dots). Open dots show the data of Ref. [10]. Full lines are the results of the fits assuming the GH parametrization for the nuclear density distribution.

In the present analysis, four different model descriptions of nuclear density distributions were used, the free parameters of which were deduced by least-square fit of the calculated to the measured cross sections. All nucleon distributions obtained, as well as the resulting root mean square radii of the distributions of protons (R_p), neutrons (R_n), core nucleons (R_c), valence nucleons (R_v), and total nuclear matter (R_m), refer to point nucleon distributions. It should be noted that, since the difference between the elementary pp and pn cross sections is relatively small, the sensitivity of the calculated p-nucleus cross section to the difference between the proton and neutron density distributions $\rho_p(r)$ and $\rho_n(r)$ is rather weak. Therefore, we did not make any difference between the one-body proton and neutron densities in the first part of our analysis. Here, we have used for the matter distribution $\rho_m(r)$ a symmetrized Fermi (SF) distribution [12] (with the "half density radius" R_0 and the diffuseness parameter a), and a Gaussian with a "halo" (GH). Both parametrizations allow for the description of an extended matter distribution as suspected for ^{6}He and ^{8}He. The GH distribution is defined by the form factor $S(t) = (1 + \alpha z^2)\exp(z)$, with $z = tR_m^2/6$, and $0 \leq \alpha \leq 0.4$. For $\alpha = 0$, the GH distribution becomes a Gaussian one, while for α close to 0.4 this distribution has a pronounced halo component. We note that the parameter R_m in the form factor is closely connected with the slope of the measured differential cross section, while the parameter α is related to the curvature of the t dependence of the cross section.

In the second part of the analysis we assumed that ^{6}He and ^{8}He nuclei consist of core nucleons (2 protons and 2 neutrons) and valence nucleons (2 neutrons for ^{6}He, and 4 neutrons for ^{8}He), described by the corresponding density distributions $\rho_c(r)$ and $\rho_v(r)$. A Gaussian (G) distribution for the core nucleon density and either a Gaussian

TABLE I. Summary of parameters obtained for various parametrizations of the model nuclear density distributions (for notations, see text; only statistical errors are given).

Nucleus	Parametrization	Parameters[a]	R_m	R_n[b]
^{4}He[c]	SF	$R_0 = 1.26(36)$, $a = 0.31(7)$	1.49(3)	⋯
	GH	$R_m = 1.49(3)$, $\alpha = 0.006(88)$	1.49(3)	⋯
^{6}He	SF	$R_0 = 1.23(54)$, $a = 0.57(7)$	2.31(6)	⋯
	GH	$R_m = 2.29(5)$, $\alpha = 0.08(5)$	2.29(5)	⋯
	GG	$R_c = 1.95(10)$, $R_v = 2.88(27)$	2.30(6)	2.46(12)
	GO	$R_c = 1.81(9)$, $R_v = 3.05(21)$	2.30(5)	2.50(10)
^{8}He	SF	$R_0 = 0.03(75)$, $a = 0.66(2)$	2.46(3)	⋯
	GH	$R_m = 2.47(4)$, $\alpha = 0.16(3)$	2.47(4)	⋯
	GG	$R_c = 1.68(7)$, $R_v = 3.04(9)$	2.46(4)	2.67(6)
	GO	$R_c = 1.42(7)$, $R_v = 3.12(7)$	2.42(3)	2.67(5)

[a] α is dimensionless, all other parameters and radii are in fm.
[b] Under the assumption of R_p equal to R_c.
[c] The parameters β_{pp} and β_{pn} were chosen to obtain $R_m = 1.49$ fm.

(G), or a 1p-shell harmonic oscillator-type density (O) for the valence nucleon density were used. We refer to these two versions of the analysis as GG and GO.

The experimental data are equally well described with the density parametrizations used, with a reduced χ^2 around unity. Solid lines in Fig. 2 show the GH case as an example. For p-^{4}He scattering, the present data and those of Ref. [10], measured in a wider t interval, were analyzed together. The results of our analysis are presented in Tables I and II, and the resulting nucleon distributions are depicted in Figs. 3 and 4. Both parametrizations (SF and GH) applied for ^{4}He have yielded identical values for the matter radius. In the case of ^{6}He and ^{8}He, the values obtained for the matter radii R_m by applying the four parametrizations mutually agree within small errors. This demonstrates that the results on the radii are quite independent on the model assumptions considered. If we account also for systematical uncertainties in the experimental data and in the analysis we finally obtain $R_m = 2.30 \pm 0.07$ fm for ^{6}He, and $R_m = 2.45 \pm 0.07$ fm for ^{8}He. In Table II these rms matter radii are compared with other experimental and theoretical results. The present values are in close agreement with those of Ref. [2]. However, other analyses [13,14] of the data on the total reaction cross sections from [2] have yielded noticeably higher values for the ^{6}He rms matter radius. We suspect that this disagreement is due to the relatively large systematical uncertainty of such an analysis.

For ^{4}He the diffuseness parameter a of the SF distribution was found to be small, and the parameter α of the GH distribution occurred to be zero within errors (see Table I). For the neutron-rich isotopes ^{6}He and ^{8}He, we note that the diffuseness parameters a are about twice as large as that for ^{4}He, and that the parameter α is larger than zero for both isotopes (most significantly in the case of ^{8}He). The nuclear matter density distributions obtained with the GG and GO parametrizations are rather similar to those obtained with the SF and GH parametrizations (see Figs. 3 and 4). This fact tells us that all versions of the present analysis agree in reproducing a rather extended matter distribution for ^{6}He and ^{8}He, the matter density decreasing with the radius much slower than in the case of ^{4}He. This result is a clear evidence for the existence of a significant neutron skin in both nuclei.

However, from our experiment alone we can deduce the information on neutron distributions only by making some assumption on the proton distributions, as it is done, for example, in our parametrizations GG and GO which suppose that protons are contained only in the core. The average values of the core radii R_c for the GG and GO parametrizations are 1.88 ± 0.12 fm for ^{6}He, and 1.55 ± 0.15 fm for ^{8}He. The different values of R_c for ^{6}He and ^{8}He may be explained by a different contribution of the valence neutrons to the center-of-mass motion of the cores in both nuclei. If we assume that R_p is equal to R_c, we obtain values of 2.48 ± 0.11 fm for ^{6}He, and

TABLE II. Nuclear matter radii R_m (in fm) for ^{6}He and ^{8}He deduced from the present experiment, compared with other experimental and theoretical results.

^{6}He	2.30(7)[a]	2.33(4) [2][b]	2.57(10) [13][b]	2.71(4) [14][b]	2.46 [15][c]	2.40 [16][c]
^{8}He	2.45(7)[a]	2.49(4) [2]			2.40 [15][c]	2.73 [17][c]

[a] This work; averaged values with total errors.
[b] These values were deduced from the same experimental data on the total reaction cross sections [2].
[c] Theoretical results.

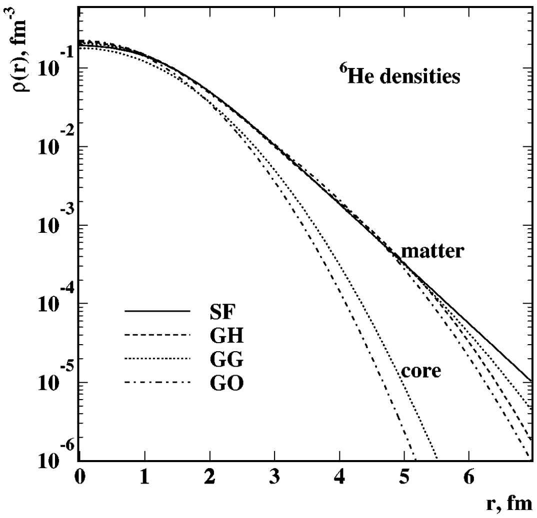

FIG. 3. Nuclear core and total nuclear matter density distributions for ^{6}He (normalized to the number of nucleons), for the different models applied (for notations see text).

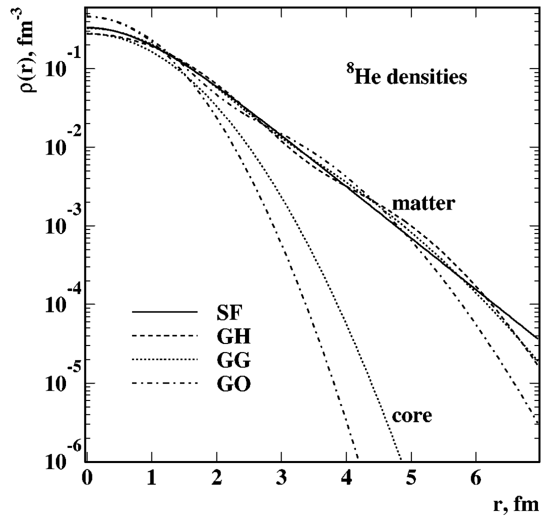

FIG. 4. Nuclear core and total nuclear matter density distributions for ^{8}He (notations are as in Fig. 3).

2.67 ± 0.05 fm for ^{8}He, for the rms radii R_n of their neutron distributions. The differences between the neutron and proton radii are accordingly 0.61 ± 0.21 fm for ^{6}He, and 1.12 ± 0.17 fm for ^{8}He.

In summary, we have investigated for the first time the proton elastic scattering on exotic nuclei at intermediate energy. Our work demonstrates that the present method is an effective means for studying the radial structure of these nuclei. The matter radii of ^{6}He and ^{8}He have been determined in a rather model independent way. The results are consistent with a pronounced neutron skin in both isotopes. For getting a less model dependent information on the radii of the neutron distributions, data on the charge radii from other experiments are needed.

This work, which in essential parts forms the subject of the Ph.D. thesis of S. R. Neumaier, was supported by the BMBF (06DA461), the Scientific and Technological Cooperation Programm between Germany and Russia, and by the Russian Fundamental Nuclear Physics Grant No. 121.04. We are grateful to Yu. Ts. Oganessyan, and E. Kankeleit for fruitful discussions, T. Beha, K-H. Behr, A. Brünle, K. Burkhard, and C. Fischer for their technical assistance in the preparation of the experimental setup, and P. Lorenzen and P. Singer for their help during the experiment. The visiting group from PNPI thanks the GSI for the hospitality.

[1] I. Tanihata, Nucl. Phys. **A488**, 113c (1988).
[2] I. Tanihata *et al.,* Phys. Lett. B **289**, 261 (1992).
[3] G. D. Alkhazov, S. L. Belostotsky, and A. A. Vorobyov, Phys. Rep. **42C**, 89 (1978).
[4] G. D. Alkhazov and A. A. Lobodenko, Pis'ma Zh. Eksp. Teor. Fiz. **55**, 377 (1992); JETP Lett. **55**, 379 (1992).
[5] S. R. Neumaier *et al.*, Nucl. Phys. **A583**, 799c (1995).
[6] S. R. Neumaier *et al.*, in *Proceedings of the International Conference on Exotic Nuclei and Atomic Masses (ENAM), Arles, France, 1995* (Editions Frontiers, Gif-sur-Yvette, France, 1995), Vol. 227.
[7] H. Geissel *et al.*, Nucl. Instrum. Methods Phys. Res., Sect. B **70**, 286 (1992).
[8] A. A. Vorobyov *et al.,* Nucl. Instrum. Methods **119**, 509 (1974).
[9] J. P. Burq *et al.*, Nucl. Phys. **B217**, 285 (1983).
[10] O. G. Grebenjuk *et al.,* Nucl. Phys. **A500**, 637 (1989).
[11] H. Devries *et al.,* At. Data Nucl. Data Tables **36**, 495 (1987).
[12] Yu. N. Eldyshev, V. N. Lukyanov, and Yu. S. Pol, Yad. Fiz. **16**, 506 (1972) [Sov. J. Nucl. Phys. **16**, 282 (1973)].
[13] L. V. Chulkov *et al.*, Europhys. Lett. **8**, 245 (1989).
[14] J. S. Al-Khalili *et al.*, Phys. Rev. C **54**, 1843 (1996).
[15] K. Varga, Y. Suzuki, and Y. Ohbayasi, Phys. Rev. C **50**, 189 (1994).
[16] A. Csoto, Phys. Rev. C **48**, 165 (1993).
[17] Y. Suzuki and K. Ikeda, Phys. Rev. C **38**, 410 (1988).